Inorganic Chemistry

Article

pubs.acs.org/IC

Chirality Transfer from Chiral Monoamines to an *m*-Phthalic Diamide-Linked Zinc Bisporphyrinate with a Benzylamide Substituent

Qingyun Hu,[†] Congcong Zhuo,[†] Yong Wang,*[,†] Chuanjiang Hu,*[,†,‡] and Jianping Lang*[,†]

[†]State and Local Joint Engineering Laboratory for Novel Functional Polymeric Materials, College of Chemistry, Chemical Engineering and Materials Science, Soochow University, Suzhou 215123, Jiangsu, P. R. China

[‡]Applied Technology College of Soochow University, Suzhou 215325, Jiangsu P.R. China

Supporting Information

ABSTRACT: An *m*-phthalic diamide-linked bisporphyrin with a benzylamide substituent has been designed and synthesized. It has two types of carbonyl groups. In the solution of this zinc bisporphyrinate, these carbonyl groups are involved in the formation of two different Zn−O coordination interactions: one is formed between neighboring zinc bisporphyrinates; another is formed within zinc bisporphyrinate. The chirality sensing abilities of this zinc porphyrinate to a number of chiral monoamines have been examined. When zinc bisporphyrinate was mixed with a series of chiral monoamines, the signs of the circular dichroism spectra for the chiral monoamines of the same handedness with an aryl group as the substituent are just opposite to those with an alkyl group as the substituent. NMR studies reveal that stepwise coordinations lead to 1:1 and 1:2 host−guest complexes. The structure of the 1:1 host−guest complex was confirmed by crystallography, it is the first time that a 1:1 host−guest complex formed between zinc bisporphyrinate and a chiral monoamine has been crystallographically characterized. The structure reveals that there is an intramolecular hydrogen bond between the amide oxygen and the coordinated NH_2. We further investigated the chirality transfer mechanism by density functional theory calculations. Our studies suggest that the interactions between the linker and guests in this bisporphyrin system are crucial in the chirality transfer process, and the nature of the bulkiest substituent of chiral monoamines makes a difference. For R-type guests, with an alkyl group, the steric repulsion makes the conformer A more energetically favorable, which leads to the anticlockwise twist and negative Cotton effect. However, with an aryl group, the $\pi-\pi$ interaction makes the conformer B more energetically favorable, which leads to the clockwise twist and positive Cotton effect.

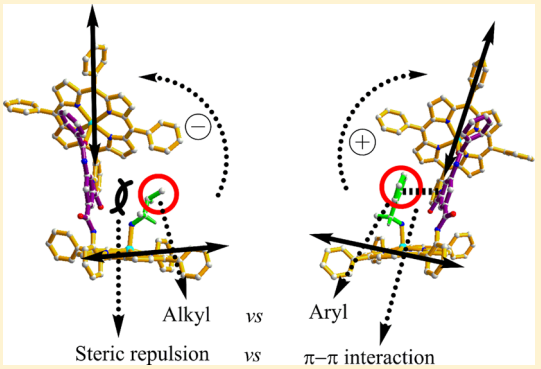

INTRODUCTION

Porphyrins have been widely used in chirality recognition, induction, and transfer in recent years.[1−5] Because porphyrins have distinct spectroscopic properties, such as a red-shifted and intense UV−vis absorption, circular dichroism (CD) spectroscopy provides a convenient method for studying porphyrin systems. Bisporphyrins have an advantage in these studies especially for chiral guests without chromophores, such as diamines, diols, and amino alcohols, because they can provide two strong chromophores. However, for monodentate guests, such as monoamines, studies are usually more difficult because there is only one coordination site. Only a limited number of porphyrin systems have been reported for chiral monoamines.[6−12] Some studies reported that these chiral guests need to be converted to their chemical derivatives before measurement.[7−9] However, a few systems can have chirality-sensing ability for monoamines without chemical derivations.[6,10−12]

In order to have effective chirality sensing, host−guest interactions generally require at least two-point fixation. Diamines or diols could provide two coordination sites to satisfy this requirement in bisporphyrin systems. However, for monoamines, it is usually more difficult because the amine group can only provide one binding site. So, (an)other interaction(s) is (are) required. For example, in the ethane-bridged bisporphyrin system developed by Borovkov and co-workers, besides the coordination interaction, the short linkage causes steric interactions between the ethyl groups of the porphyrin and the substituents of the ligand, which result in the induced supramolecular chirality.[6,10,11] For the biphenol-bridged metal-free bisporphyrin system developed by Borhan and co-workers, there are both hydrogen-bonding and steric interactions between the monoamines and host molecule, which leads to stereodifferentiation.[12]

It is still a great challenge to design bisporphyrin systems suitable for chiral monoamines that can lead to two-point or multipoint interactions between the hosts and guests. If the linker in the bisporphyrin is close to the coordination site, there will also be interactions between the linker and guest when the

Received: March 30, 2017

DOI: 10.1021/acs.inorgchem.7b00815
Inorg. Chem. XXXX, XXX, XXX−XXX

Scheme 1. Synthetic Route for Compound III and Its Zinc Complex

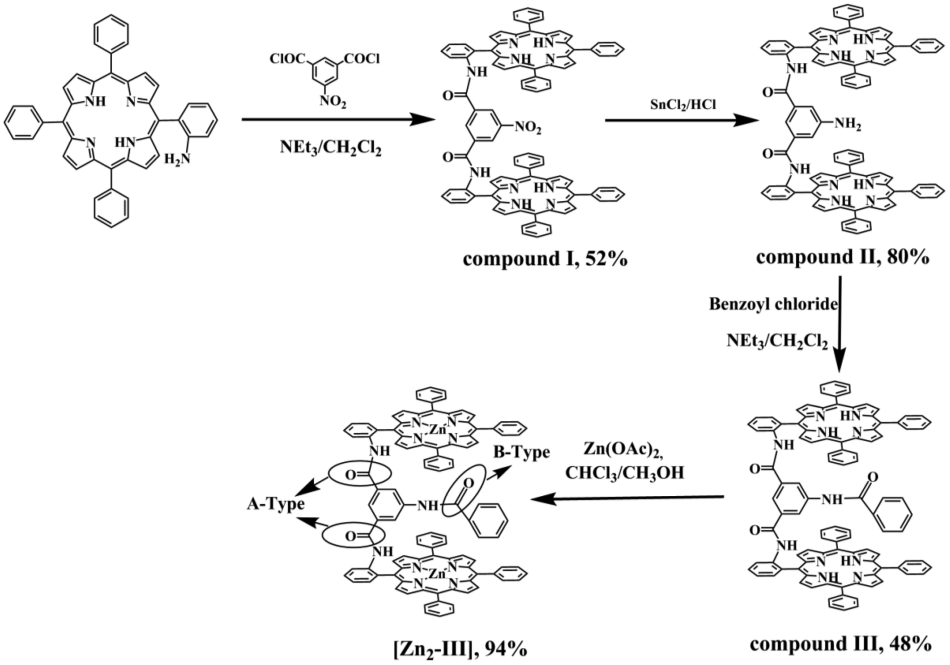

guest is coordinated to the metalloporphyrin. That could provide two-point or multipoint interactions. Then the chirality could be transferred from the guest to the corresponding host–guest complexes.

We have been working on this in recent years and have recently developed several amide-linked zinc bisporphyrins and trisporphyrinate.[13−17] These have all shown chirality transfer ability from chiral monoamines to their host–guest complexes. In the case of zinc trisporphyrinate, we obtained the crystal structure of its 1:3 host–guest complex, and the crystal structure reveals that the porphyrin subunits adopt a trans configuration. However, it is difficult to explain the corresponding chirality transfer mechanism for such a multichromophore system in low symmetry. On the other hand, for the zinc bisporphyrinate system having only two porphyrin subunits, the corresponding chirality transfer mechanism could be relatively easy to investigate. However, our previous studies did not get any crystal structures of their host–guest complexes for the bisporphyrin system, so we did not obtain an accurate host–guest binding mode. Herein, in order to obtain more insight on the chirality transfer mechanism for these systems, we have designed and synthesized the bisporphyrin **III**, as shown in Scheme 1. The bisporphyrin **III** is derived from *m*-phthalic diamide-linked bisporphyrin, and it has both features of previously studied amide-linked bisporphyrin and trisporphyrin: two porphyrin subunits and three amide groups. These amide groups can be classified as types A and B, which could have different roles in the chirality transfer process. We have studied their chiral-sensing abilities to five chiral monoamines (3-methyl-2-butylamine, the guest **1**; 3,3-dimethyl-2-butylamine, the guest **2**; 1-cyclohexylethylamine, the guest **3**; 1-phenylethylamine, the guest **4**; 1-(2-naphthyl)ethylamine, the guest **5**). We obtained the crystal structure of the host–guest crystal structure of [Zn_2-**III**]·**1R**. Further investigation on the chirality transfer mechanism was made by UV–vis and NMR spectroscopy and density functional theory (DFT) calculations.

EXPERIMENTAL SECTION

Material and Physical Methods. All reagents were obtained from commercial sources without further purification unless otherwise noted. Triethylamine (Et_3N) was distilled over potassium hydroxide, and methylene chloride was treated with CaH_2 before use. Zinc 5-(2-aminophenyl)-10,15,20-triphenylporphyrinate was synthesized according to reported methods.[14] Elemental analyses (carbon, hydrogen, and nitrogen) were performed with an Elementar Vario EL III analytical instrument. ^{1}H NMR spectra were recorded at room temperature, using an Agilent 400 MHz spectrometer in $CDCl_3$ with tetramethylsilane (TMS) as the internal standard; chemical shifts are expressed in ppm relative to TMS (0 ppm). Two-dimensional NMR spectra were recorded on a Bruker AVANCE 600 MHz NMR instrument. UV–vis spectra were recorded with a Shimadzu UV-3150 spectrometer. CD spectra were recorded on a PMT model J-815 spectropolarimeter at 298 K. Scanning conditions were as follows: date pitch = 0.2 nm; bandwidth = 2 nm; response time = 1 s; scanning speed = 50 nm/min.

CD and UV–Vis Measurements. UV–vis titration experiments were carried out as follows. Measurements were performed by adding different aliquots of the optically active monoamine solution to the host solution in methylene chloride at room temperature. Then UV–vis spectra were recorded after each addition.

For CD measurements, the background spectrum was taken from 380 to 460 nm with a scan rate of 100 nm/min at 25 °C. A zinc bisporphyrinate solution was injected into a 1.0 cm quartz cuvette. Then guests were added to the above solution to form the corresponding complexes. CD spectra were measured after several minutes. The resultant CD spectra recorded in millidegrees were normalized on the basis of the concentrations of zinc bisporphyrinates.

A solid CD spectrum was measured with the following method: KBr pellets were prepared by grinding a single crystal sample with solid KBr and applying great pressure to the dry mixture. The thickness of the KBr pellet was about 0.3 mm. The CD spectrum was then recorded.

^{1}H NMR Titrations. For ^{1}H NMR titration experiments, portions of a solution of chiral monoamine in $CDCl_3$ were added to the solution of [Zn_2-**III**] in $CDCl_3$ in a 5-mm-o.d. NMR tube, and NMR spectra were recorded after each addition.

Preparation of the Free Base Bisporphyrin I. A solution of 5-nitroisophthalic acid (0.069 g, 0.36 mmol) in thionyl chloride (8 mL)

DOI: 10.1021/acs.inorgchem.7b00815
Inorg. Chem. XXXX, XXX, XXX−XXX

was refluxed under nitrogen for 4 h, followed by the removal of excess reagent under reduced pressure. The residual white solid was redissolved in CH_2Cl_2 (30 mL), and Et_3N (150 μL, 1.1 mmol) was added to the solution described above and stirred for 10 min in an ice bath. Zinc 5-(2-aminophenyl)-10,15,20-triphenylporphyrinate (0.50 g, 0.78 mmol) was added to the solution under a nitrogen atmosphere overnight in an ice bath. Then it was washed with water, and the organic layer was collected and evaporated to dryness under vacuum. A purple solid was obtained and purified by silica gel chromatography (pure CH_2Cl_2; 0.27 g, 52% yield). ^{1}H NMR (400 MHz, $CDCl_3$): δ 8.82 (d, J = 8.9 Hz, 8H), 8.71 (d, J = 4.4 Hz, 4H), 8.53 (d, J = 4.5 Hz, 4H), 8.18 (d, J = 7.4 Hz, 6H), 8.10 (dd, J = 16.4, 7.0 Hz, 8H), 7.96 (d, J = 7.4 Hz, 2H), 7.83−7.76 (m, 6H), 7.71 (dd, J = 12.7, 6.9 Hz, 10H), 7.61 (t, J = 6.9 Hz, 4H), 7.49 (t, J = 7.5 Hz, 2H), 7.30 (s, 2H), 6.62 (s, 2H), 6.58 (s, 1H), −2.91 (s, 4H). ^{13}C NMR (151 MHz, DMSO): δ 163.71, 145.79, 141.55, 138.32, 136.42, 136.32, 136.28, 134.66, 134.50, 134.37, 132.18, 131.64, 129.37, 128.46, 128.33, 127.39, 127.28, 127.21, 126.43, 125.43, 123.28, 120.64, 120.13, 116.10, 40.39, 40.25, 40.11, 39.97, 39.84, 39.70, 39.56, 31.36, 22.47, 14.37. UV−vis [CH_2Cl_2; λ_{max}, nm (log ε, cm^{-1} M^{-1})]: 418 (5.86), 517 (4.59), 553 (4.07), 594 (4.16). Anal. Calcd for $C_{96}H_{63}N_{10}O_4$: C, 81.17; H, 4.47; N, 9.86. Found: C, 81.20; H, 4.50; N, 9.88.

Preparation of the Free Base Bisporphyrin II. The free base bisporphyrin **I** (0.50 g, 0.35 mmol) was dissolved in 20 mL of concentrated HCl, and 2.3 g of $SnCl_2{\cdot}2H_2O$ was added. The bright-green solution was stirred at room temperature for 45 min and then heated at 65 °C for 30 min. After the solution was cooled in an ice bath, concentrated ammonia was added to bring the suspension to pH 10. The brown-violet mixture was stirred for 1 h with 50 mL of $CHC1_3$. The organic layer was separated, washed twice with water, and dried over Na_2SO_4. After filtration, the solvent was removed on a rotary evaporator. The purple solid was obtained and purified by column chromatography (silica, pure CH_2Cl_2; 0.39 g, 80% yield). ^{1}H NMR (400 MHz, DMSO): δ 8.92 (s, 2H), 8.74 (t, J = 22.5 Hz, 8H), 8.62 (s, 8H), 8.19 (s, 2H), 8.13 (s, 6H), 8.04 (t, J = 9.9 Hz, 4H), 7.98 (d, J = 6.9 Hz, 2H), 7.82 (d, J = 6.2 Hz, 6H), 7.77 (s, 8H), 7.66 (s, 6H), 7.61−7.55 (m, 2H), 7.52 (d, J = 7.7 Hz, 2H), 5.66 (s, 1H), 5.54 (s, 2H), 3.90 (s, 2H), −3.02 (s, 4H). ^{13}C NMR (151 MHz, DMSO): δ 166.04, 147.23, 141.63, 141.58, 138.77, 136.27, 135.77, 135.36, 134.56, 131.56, 129.18, 128.50, 128.37, 127.43, 127.33, 126.00, 124.63, 120.62, 120.10, 116.27, 114.39, 113.06, 40.37, 40.23, 40.09, 39.96, 39.82, 39.68, 39.54. UV−vis [CH_2Cl_2; λ_{max}, nm (log ε, cm^{-1} M^{-1})]: 417 (5.77), 517 (4.05), 551 (3.82), 529 (3.96). Anal. Calcd for $C_{96}H_{65}N_{10}O_2$: C, 82.92; H, 4.71; N, 10.07. Found: C, 82.95; H, 4.74; N, 10.09.

Preparation of the Free Base Bisporphyrin III. The reaction was performed under anaerobic conditions. The free base bisporphyrin **II** (0.50 g, 0.36 mmol) was dissolved in anhydrous methylene chloride (50 mL). Et_3N (150 μL, 1.07 mmol) was added to the solution described above, the mixture was stirred for 15 min in an ice bath, and then benzoyl chloride (46 μL, 0.40 mmol) was added. The mixture was slowly warmed to room temperature, and the reaction was monitored by thin-layer chromatography (TLC). After 8 h, the reaction was complete. The solution was rotor-evaporated to dryness under vacuum. The purple solid was obtained and purified by column chromatography (silica, pure CH_2Cl_2; 0.26 g, 48% yield). ^{1}H NMR (400 MHz, $CDCl_3$): δ 8.88−8.79 (m, 4H), 8.76 (d, J = 4.0 Hz, 4H), 8.69 (d, J = 4.0 Hz, 4H), 8.55 (d, J = 3.7 Hz, 4H), 8.25−8.15 (m, 6H), 8.11 (s, 4H), 7.99 (d, J = 6.7 Hz, 4H), 7.88 (d, J = 7.4 Hz, 2H), 7.83−7.73 (m, 6H), 7.69 (s, 10H), 7.54 (s, 4H), 7.44 (t, J = 7.4 Hz, 2H), 7.39 (s, 2H), 7.06 (t, J = 7.3 Hz, 1H), 6.54 (t, J = 7.5 Hz, 2H), 6.24 (s, 1H), 6.16 (s, 2H), 5.78 (s, 1H), 5.67 (d, J = 7.6 Hz, 2H), −2.86 (s, 4H). ^{13}C NMR (151 MHz, DMSO): δ 163.54, 163.34, 142.13, 141.75, 138.03, 137.43, 135.09, 135.03, 134.72, 134.59, 134.51, 132.63, 131.95, 130.97, 129.38, 127.89, 127.72, 127.70, 126.83, 126.76, 126.60, 125.71, 123.07, 120.97, 120.93, 120.69, 120.57, 119.45, 112.64, 77.28, 77.07, 76.86. UV−vis [CH_2Cl_2; λ_{max}, nm (log ε, cm^{-1} M^{-1})]: 417 (5.53), 515 (4.10), 552 (3.16), 590 (2.54). Anal. Calcd for $C_{103}H_{69}N_{10}O_3$: C, 82.77; H, 4.65; N, 9.37. Found: C, 82.81; H, 4.68; N, 9.32.

Preparation of [Zn_2-III]. The free base bisporphyrin **III** (0.50 g, 0.33 mmol) was dissolved in a mixture of $CHCl_3$ (150 mL) and CH_3OH (50 mL). $Zn(CH_3COO)_2$ (0.24 g 1.32 mmol) was added to the solution described above and refluxed for 2 h. Then it was extracted with water, and the organic layer was collected and evaporated to dryness under vacuum. The purple solid was obtained and purified by silica gel chromatography (99:1 CH_2Cl_2/methanol; 0.51 g, 94% yield). ^{1}H NMR (400 MHz, $CDCl_3$): δ 8.85 (s, 8H), 8.61 (d, J = 4.3 Hz, 4H), 8.37 (d, J = 4.3 Hz, 4H), 8.19 (s, 6H), 8.04 (d, J = 6.9 Hz, 2H), 7.91 (d, J = 7.3 Hz, 2H), 7.85−7.72 (m, 8H), 7.66 (d, J = 16.4 Hz, 10H), 7.49 (t, J = 7.5 Hz, 8H), 7.09 (s, 3H), 6.82 (s, 2H), 6.56 (t, J = 7.4 Hz, 2H), 5.79 (s, 1H), 5.06 (s, 2H), 4.18 (d, J = 7.5 Hz, 2H), 3.78 (s, 1H). ^{13}C NMR (151 MHz, DMSO): δ 161.38, 150.18, 149.91, 149.13, 146.06, 146.04, 145.42, 142.92, 137.62, 135.43, 134.42, 134.01, 133.46, 132.58, 132.01, 131.89, 130.83, 130.48, 130.04, 128.94, 127.45, 127.17, 126.34, 126.22, 123.91, 123.49, 121.48, 120.90, 120.24, 119.26, 118.11, 112.14, 96.90, 93.15, 77.19, 76.98, 76.77, 31.57, 29.67, 14.10, 1.01. UV−vis [CH_2Cl_2; λ_{max}, nm (log ε, cm^{-1} M^{-1})]: 422 (5.60), 556 (4.21), 597 (3.04). Anal. Calcd for $C_{103}H_{65}N_{10}O_3Zn_2$: C, 76.30; H, 4.04; N, 8.64. Found: C, 76.35; H, 3.99; N, 8.69.

Preparation of Crystals of [Zn_2-III]·1R. [Zn_2-**III**] (50 mg, 0.030 mmol) was dissolved in CH_2Cl_2 (1 mL), 200 μL of a 0.2 M solution of (*R*)-2-amino-3-methylbutane in anhydrous CH_2Cl_2 was added to the solution described above, and the mixture was stirred for ∼3 min. Then it was transferred to 8 mm × 250 mm glass tubes. *n*-Hexane was added as a nonsolvent at room temperature. After 3 months, purple crystals were obtained, which were then isolated by filtration, washed with *n*-hexane, and dried under vacuum. (11 mg, 21% yield). Anal. Calcd for $C_{108}H_{78}N_{11}O_3Zn_2$: C, 75.92; H, 4.60; N, 9.02; Found: C, 75.82; H, 4.65; N, 9.05.

X-ray Structure Determination. The measurements of single crystals were performed on a Bruker APEX-II CCD X-ray diffractometer by using graphite-monochromated Mo Kα (λ = 0.71073 nm). The structure was determined by direct methods and refined on F^2 using the full-matrix least-squares method with *SHELXTL*, version 2014.[18] All non-hydrogen atoms were refined anisotropically; all hydrogen atoms were theoretically added and rode on their parent atoms. In the structure, the asymmetric unit contains badly disordered solvent molecules. *SQUEEZE*[19] was used to model all disordered solvates. The electron count within the interporphyrin voids was 825e for [Zn_2-**III**]·**1R** (corresponding roughly to five molecules of methylene chloride per [Zn_2-**III**]). Details of the crystal parameters, data collection, and refinements are summarized in Table 1. Complete crystallographic details, atomic coordinates, anisotropic thermal parameters, and fixed hydrogen-atom coordinates are given in the CIF file (CCDC 1531702).

Computational Methods. All calculations are on the basis of the crystal structural data. To simplify the calculations, we only consider a single bisporphyrin molecule, and we did not calculate the aggregated species. We first performed DFT calculations on the free host [Zn_2-**III**]. Then we did calculations on the corresponding 1:1 ([Zn_2-**III**]·**1R** and [Zn_2-**III**]·**4R**) and 1:2 ([Zn_2-**III**]·(**1R**)$_2$ and [Zn_2-**III**]·(**4R**)$_2$) complexes. Full optimizations on these structures were performed by DFT at the level of B3LYP/6-31G* using the *Gaussian09* suite of programs.[20] We employed DFT with no symmetry constraints to investigate the optimized geometries.

RESULTS AND DISCUSSION

CD Spectral Studies. In this study, five types of chiral monoamines were used as guests, and they have different substituents X. Each host and each enantiopure amine were mixed in methylene chloride, and the corresponding CD spectra were recorded. Because the formation constants for binding monoamines to zinc porphyrinates are in general around 10^3 L/mol[21] and the concentrations of porphyrin used in our CD measurements are around 10^{-6} mol/L, a large excess of guests are required to completely convert the host to the corresponding host−guest complex. In our experiments, more

DOI: 10.1021/acs.inorgchem.7b00815
Inorg. Chem. XXXX, XXX, XXX−XXX

Table 1. Crystal Data and Structural Refinement Data of [Zn_2-III]·1R

crystal	[Zn_2-III]·1R
chemical formula	C_{108} H_{78} N_{12} O_3 Zn_2
fw	1722.56
wavelength (Å)	0.71073
temperature (K)	223(2)
cryst syst	monoclinic
space group	*C*2
a (Å)	36.298(3)
b (Å)	15.1343(11)
c (Å)	26.262(2)
α (deg)	90
β (deg)	133.414(4)
γ (deg)	90
V (Å^3)	10479.7(15)
Z	4
density (Mg/m^3)	1.092
abs coeff (mm^{-1})	0.509
F(000)	3576.0
data collection θ range (deg)	2.41−27.51
index ranges	$-47 \le h \le 47$, $-19 \le k \le 19$, $-34 \le l \le 34$
reflns collected	301609
R_{int}	0.0622
indep reflns	24236
data/restraints/param	24236/92/1181
GOF on F^2	1.024
R1[a] [$I > 2\sigma(I)$]	0.0346
wR2	0.0871
peak/hole (e/Å^3)	0.491/−0.462
Flack parameter	0.032(6)

[a] $R1 = (F_o - F_c)/F_o$; $wR2 = w(F_o^2 - F_c^2)^2/w(F_0^2)^2]^{1/2}$.

than 1000 equiv of guests was generally used. Their titration CD spectra and the corresponding plots of the CD intensity as a function of the equivalents of guests are provided in the Supporting Information. These figures show that the CD intensities reached a maximum at a large excess of guests, which suggested that all zinc bisporphyrinates were converted to the corresponding host−guest complexes. The spectra in Figure 1 show clear signals with typical bisignate Cotton effects in the Soret band region. The CD spectral data are listed in Table 2. These results reveal the following features: (1) For a pair of enantiomers of chiral amines, the CD spectra showed similar shapes and intensities but opposite signs. (2) More importantly, when the substituent X is an aryl group or an alkyl group, the signs of the resulting CD are different. For the R-type chiral monoamines, when X is an alkyl group, such as **1R**, **2R**, and **3R**, the longer-wavelength peak of the Soret band is negative and the shorter-wavelength peak is positive. However, when X is an aryl group, such as **4R** and **5R**, the signs of CD are just opposite to those with X as an alkyl group. As follows, we have investigated the chirality transfer mechanism through UV−vis spectra, NMR studies, the crystal structure, and DFT calculations.

UV−vis Spectral Studies and Self-Aggregation Process for the Host. UV−vis spectra of [Zn_2-**III**] were measured at different concentrations, as shown in Figure 2. The spectra of [Zn_2-**III**] show one strong Soret band at 421 nm and one shoulder at 431 nm, which are similar to those reported for *m*-phthalic diamide-linked zinc bisporphyrinates[14] but different from those for the oxalic amide-linked species.[13] For comparison, the free base bisporphyrin **III** was also measured by UV−vis spectroscopy. The spectrum is provided in Figure S11, which does not show such a shoulder. This suggests that zinc is involved in the formation of such a shoulder. Generally, the coordination of zinc porphyrin to oxygen or nitrogen leads to bathochromic shifts compared to four-coordinate zinc porphyrins.[22] In our case, such a shoulder at longer wavelength could be caused by the Zn−O coordination interactions.

As shown in Figure 2, when the concentration of [Zn_2-**III**] increased, the intensity of the shoulder increased, and the intensity of the peak at 421 nm deceased. Such a concentration-dependent spectral change suggests that the Zn−O bond is formed between neighboring zinc bisporphyrinates, and aggregation through the coordination interactions occurs in solution. Such a coordination mode was actually found in our previous studies.[14,16] So, the following equilibrium (1) exists in solution. [Zn_2-**III**]$_n$ is the aggregated species, and [Zn_2-**III**] is the single zinc bisporphyrinate molecule.

$$[Zn_2\text{-}\mathbf{III}]_n \rightleftharpoons n[Zn_2\text{-}\mathbf{III}] \quad (1)$$

UV−vis spectroscopic titrations also have been performed between [Zn_2-**III**] and five chiral monoamines. A representative example of the spectral change of [Zn_2-**III**] induced by the addition of **1R** is shown in Figure 3. (Others are provided in Figures S12−S15.) Before the addition, the spectrum of [Zn_2-**III**] shows one strong Soret band at 421 nm and one shoulder at 431 nm. During the titration, the electronic spectra showed that the intensity of the band at 421 nm decreased and the intensity at 431 nm increased with increasing the ligand concentrations.

When guests are mixed with zinc bisporphyrinate, the following two equilibria could be in the solution because there are two zinc binding sites:

$$[Zn_2\text{-}\mathbf{III}] + L \overset{K_1}{\rightleftharpoons} [Zn_2\text{-}\mathbf{III}]\cdot L \quad (2)$$

$$[Zn_2\text{-}\mathbf{III}]\cdot L + L \overset{K_2}{\rightleftharpoons} [Zn_2\text{-}\mathbf{III}]\cdot (L)_2 \quad (3)$$

where L represents a guest.

However, because of the self-aggregation process [equilibrium (1)] in solution, the equilibria in solution became more complicated. The binding constants for the above two equilibria are difficult to determine. In fact, in the titration spectra, we did not observe clear isosbestic points. This is possibly due to the self-aggregation process. Self-aggregation through Zn−O bonds is further confirmed by NMR studies.

NMR Studies. For the free base bisporphyrin **III** and its complex [Zn_2-**III**], the ^{1}H NMR spectra are presented in Figure 4. In this bisporphyrin, all protons are aromatic protons except the NH protons. The resonances for the aromatic protons are generally located in the 7−9 ppm region.[16] However, for the bisporphyrin **III** and its complex [Zn_2-**III**], some resonances are located in the 3−7 ppm region. Because the linker is between two porphyrin subunits, the ring current effect of porphyrin could cause such upfield shifts. So, these resonances are assigned to the protons of the linker. Detailed assignments are based on ^{1}H and ^{1}H−^{1}H COSY NMR, which are presented in the Supporting Information. Compared with the free base bisporphyrin **III**, most signals for the zinc bisporphyrinate [Zn_2-**III**] remain unchanged, while the resonances of H12, H(14,16), and H(22,26) shift remarkably upfield to 3.80, 5.08, and 4.28 ppm, respectively. Such upfield shifts suggest that these protons are even much closer to the

DOI: 10.1021/acs.inorgchem.7b00815
Inorg. Chem. XXXX, XXX, XXX−XXX

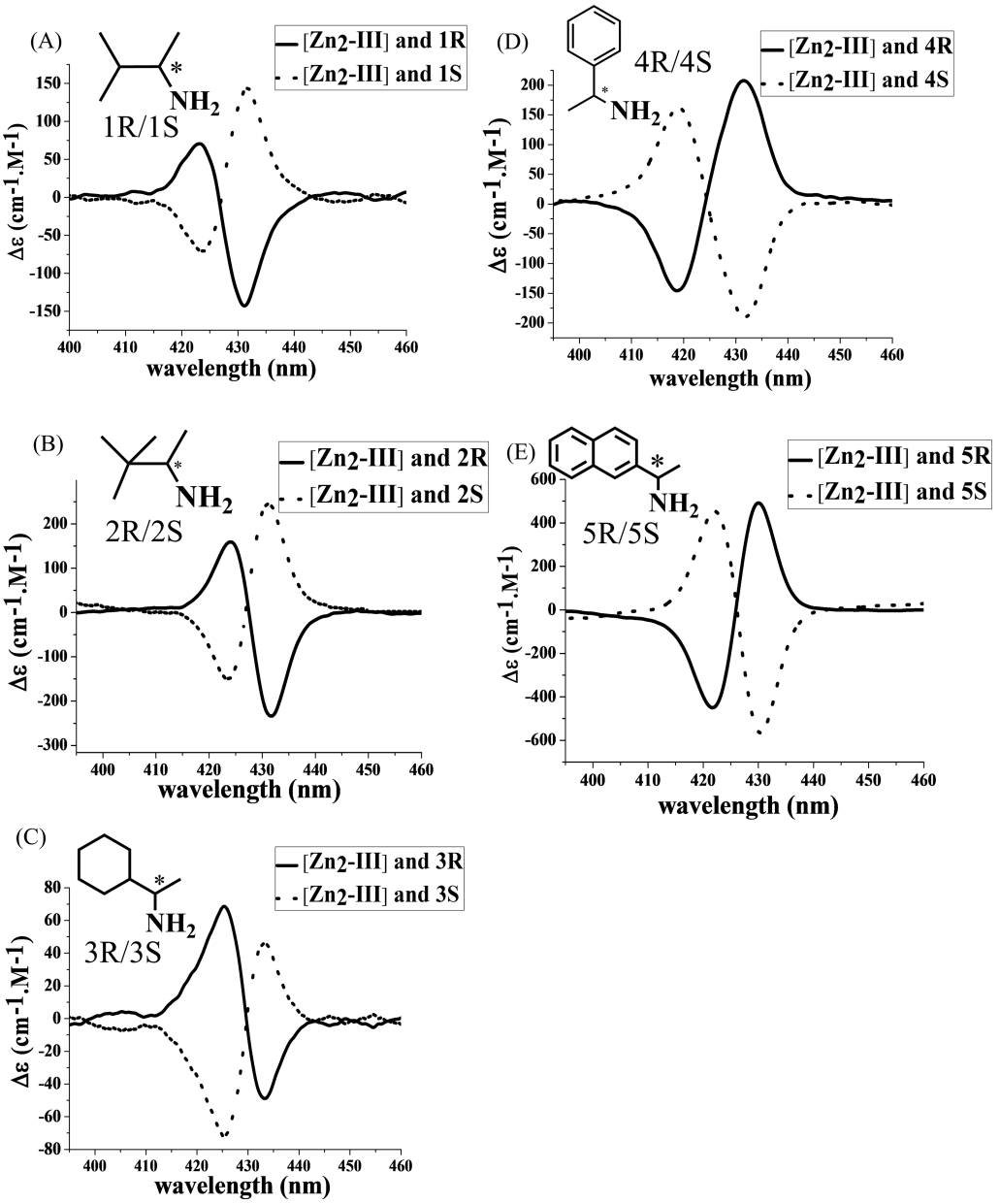

Figure 1. CD spectra of a solution of [Zn_2-**III**] (1.75×10^{-6} mol/L) and a large excess of guests in methylene chloride at 298 K. (A) 2500 equiv of **1S**, (dashed line) or **1R** (solid line); (B) 1600 equiv of **2S** (dashed line) or **2R** (solid line); (C) 1535 equiv of **3S** (dashed line) or **3R** (solid line); (D) 1340 equiv of **4S** (dashed line) or **4R** (solid line); (E) 1550 equiv of **5S** (dashed line) or **5R** (solid line).

porphyrin plane in zinc bisporphyrinate than in free base bisporphyrin, which could be due to coordination of the carbonyl oxygen atom to the neighboring zinc porphyrinate. In addition, ^{1}H NMR spectra at different concentrations have also been measured. In these spectra, most resonances do not change, but the resonance of H12 shows slight shifts.

On the basis of these NMR spectral changes, we proposed one possible mode for the self-aggregation of [Zn_2-**III**], as shown in Figure 5. In the structural formula, there are two types of carbonyl groups. In solution, both carbonyl oxygen atoms are coordinated to zinc: the A-type carbonyl group involves "intermolecular" interactions; the B-type carbonyl group involves "intramolecular" Zn−O coordination interactions. Such coordination interactions cause H12, H(14,16), and H(22,26) to locate above the adjacent porphyrin plane, and the ring current effect causes their resonances to shift upfield compared with the free base bisporphyrin.

As is also shown in Figure 5, when the B-type carbonyl oxygen atom is coordinated to zinc, coordination interactions lead to the adjacent phenyl ring above the plane of the subunit P1. H22 and H26 are closer to the shielding cone of the porphyrin ring than H23 and H25, which is similar to that in the crystal structure of [Zn_2-**III**]·**1R** (vide infra). As a result, the resonances of H22 and H26 shift more upfield than those of H23 and H25.

On the other hand, "intermolecular" interactions are concentration-dependent, while "intramolecular" interactions are not. When we change the concentrations, the resonances of these protons behave differently. The proton H12 is close to the A-type carbonyl group, and "intermolecular" interactions lead to its shift upon changes in the concentration. On the

DOI: 10.1021/acs.inorgchem.7b00815
Inorg. Chem. XXXX, XXX, XXX−XXX

Table 2. Observed CD Spectral Data of the Complexes of [Zn_2-III] (1.75×10^{-6} M) with Chiral Monoamines[a] in Methylene Chloride at 298 K

	λ_{max}, nm ($\Delta\varepsilon$, cm^{-1} M^{-1})		
	first cotton	second cotton	A_{obs}[b]
1R	432 (−142)	423 (+70)	−212
1S	431 (+143)	421 (−68)	+211
2R	431 (−234)	424 (+160)	−394
2S	431 (+248)	423 (−150)	+398
3R	433 (−50)	425 (+68)	−118
3S	433 (+53)	424 (−70)	+123
4R	431 (+197)	419 (−160)	+357
4S	431 (−193)	419 (+163)	−356
5R	430 (+498)	422 (−452)	+950
5S	429 (−483)	420 (+443)	−926

[a]The corresponding host−guest ratios are the same as those in Figure 1. [b]$A_{obs} = \Delta\varepsilon_1 - \Delta\varepsilon_2$. This value represents the total amplitude of the experimentally observed CD couplets.

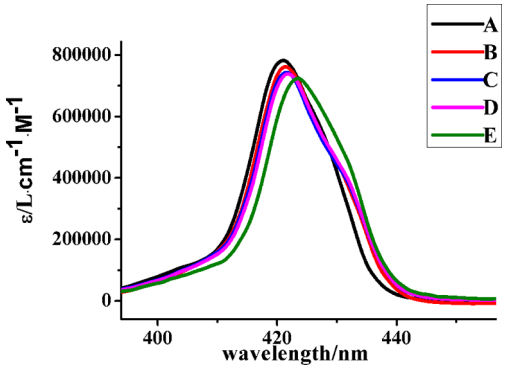

Figure 2. UV−vis spectra of [Zn_2-III] in 0.1 mm, 1 mm, and 1.0 cm quartz cells at different concentrations in methylene chloride. The intensities are normalized on the basis of the concentrations of [Zn_2-III]: (A) 1.5×10^{-7} mol/L; (B) 6.0×10^{-7} mol/L; (C) 1.5×10^{-6} mol/L; (D) 1.5×10^{-5} mol/L; (E) 1.5×10^{-4} mol/L.

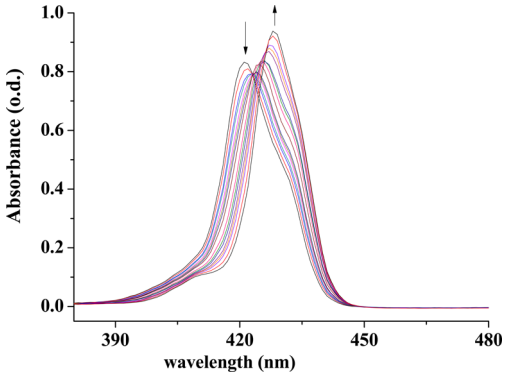

Figure 3. UV−vis spectral change of [Zn_2-III] (1.50×10^{-6} M) upon the addition of **1R** as the host−guest molar ratios are from 1:0 to 1:850.

other hand, the protons close to the B-type carbonyl group, such as H24, H(22,26), and H(23,25), do not show clear shifts because the B-type carbonyl group involves "intramolecular" Zn−O coordination interactions. "Intermolecular" interactions can result in self-aggregation, as shown in equilibrium (1), which may lead to the formation of a dimer, trimer, or even polymer. It is likely that there are several aggregated species with different "*n*" values in solution, and there could also be equilibria between them, which makes the equilibria more complicated in solution.

^{1}H NMR titration experiments were performed between [Zn_2-III] and **1R**. When the guest was added to the [Zn_2-III] solution, there were some resonances located in the −4 to 0 ppm region, as shown in Figure S20, which is similar to our studies on previously reported amide-linked bisporphyrin systems. Obviously, the large upfield shifts of these protons are due to coordination of the guests to zinc porphyrinate. The detailed titration spectra shown in Figure 6 gave us more information on the coordination interactions. During titration, the resonances of the protons of the linker in the host have shown remarkable shifts. When the host−guest ratio is below 1:1, the resonance of H12 has the largest shift; when the ratio is over 1:1, the resonance of H(22,26) has the largest shift. When the guest is in a large excess, the resonance pattern is very similar to that of the free base porphyrin **III**. This suggests that the NMR spectral changes during titration are caused by replacing the Zn−O bonds with the Zn−N (from amine) bonds. While the structural formula suggests that H12 is close to the A-type carbonyl, H(22,26) is close to the B-type carbonyl. The above studies suggest that, during titration, the A-type carbonyl oxygen atom was first replaced by one monoamine to form the 1:1 complex, and then the B-type carbonyl oxygen atom was replaced by another monoamine to form the 1:2 host−guest complex.

The ^{1}H NMR titration experiments were also performed between [Zn_2-III] and **4R**. Their spectra (Figure S22) show changes similar to those for **1R**. This suggests that **4R** is also coordinated to [Zn_2-III] in a stepwise fashion, leading to the formation of 1:1 and 1:2 host−guest complexes during titration.

On the basis of the ^{1}H NMR titration results, Job plots for the titration of **1R** or **4R** into a [Zn_2-III] solution are shown in Figures S23 and S24. The plots showed a broad peak around 0.3−0.5 mole fraction but not at 0.33, as was expected for a 1:2 host−guest complex. This is possibly due to the limitation of Job plots. Actually, there were some reports on the limited applicability of this method.[23−25] Because there are several equilibria and too many species (including the aggregated species) in solution, the Job plot method is not suitable for this system.

X-ray Crystal Structure of [Zn_2-III]·1R. In order to understand the chirality transfer mechanism, we need to obtain the binding mode of the host−guest complexes. One of the best ways to get the binding mode is through the crystal structure. We tried to obtain crystal structures for the host−guest complexes. For one of the alkyl-substituted guests, **1R**, we obtained single crystals of [Zn_2-III]·**1R**.

The structure of [Zn_2-III]·**1R** was solved in a chiral space group, C2. One asymmetric unit contains one zinc bisporphyrinate molecule. The bisporphyrin host molecule has two zinc porphyrinate subunits that are linked by an *m*-phthalic diamide group. Interestingly, both zinc atoms are five-coordinate, but their axial ligations are different. As shown in Figure 7, for the subunit P1, the axial ligand is the N1 atom of the chiral guest. The ligand adopts an "inside" binding mode (the ligand is facing the linker). For the subunit P2, the axial ligation is from the B-type carbonyl oxygen O013 of the amide group of the linker. Because of coordination, the phenyl rings composed of C21, C22, C23, C24, C25, and C26 are over the plane of the porphyrin subunit P2, and C22/C26 and their

DOI: 10.1021/acs.inorgchem.7b00815
Inorg. Chem. XXXX, XXX, XXX−XXX

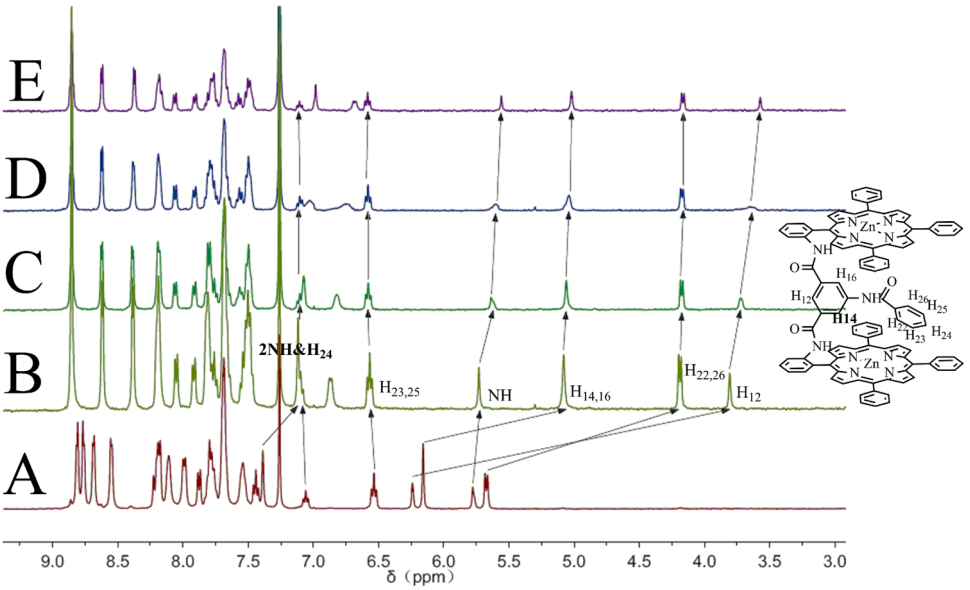

Figure 4. ^{1}H NMR spectra for compound **III** (A; 3.3×10^{-3} M) and [Zn_2-**III**] at different concentrations: (B) 4.6×10^{-3} M; (C) 1.2×10^{-3} M; (D) 0.92×10^{-3} M; (E) 0.45×10^{-3} M. The inset shows the proton numbering scheme of the linker in the host. The arrows show the shifts of the relevant protons.

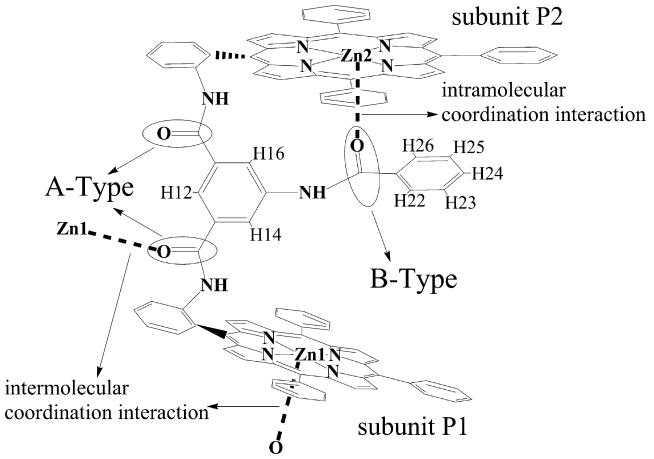

Figure 5. Proposed binding mode for [Zn_2-**III**]. The A-type carbonyl group involves "intermolecular" interactions, and the B-type carbonyl group involves "intramolecular" Zn−O coordination interactions.

protons H22/H26 are closer to the porphyrin center than C23/C25 and H23/H25 (vide supra). So, this coordination mode is consistent with our NMR studies. Besides the coordination interaction, the guest **1R** also involves hydrogen-bonding interactions. There is an intramolecular hydrogen bond between N1 and the carbonyl oxygen O012. The corresponding distance N1···O012 is 2.919(4) Å, and the bond angle N1−H1B···O012 is 159°. These interactions could be the major factors stabilizing the "inside" binding mode for the 1:1 complex.

The C5−C15−C5′−C15′ torsion angle can be used to present the dihedral angle between the two transition moments of the chromophores for the effective exciton coupling interactions in the bisporphyrin system.[26,27] In this structure, two porphyrin subunits form an anticlockwise twist with the C5−C15−C5′−C15′ torsion angle (here it is C1M3−C1M1−C2M1−C2M3) of −147°. On the basis of the exciton chirality method,[28] the anticlockwise twist will lead to a negative Cotton effect. This is consistent with our experimental results.

Solid-State CD Spectrum. For [Zn_2-**III**]·**1R**, we also did CD measurements on several single-crystal samples. For these measurements, the signals were all weak. However, they did show CD signals in the Soret band region. One of them is given in Figure 8. The CD spectrum shows the same sign and similar shape as the solution CD spectra. This confirms the chirality of the single crystal.

Computational Studies on the Chirality Transfer Mechanism. In order to gain more insight into the chirality transfer mechanism for this system, we did further investigations by DFT calculations. On the basis of the crystal structure, we did calculations on the host, 1:1 and 1:2 host−guest complexes for the guests **1R** and **4R**. All of the optimized structures are displayed in Figures 9 and 10. We found that, in all of these optimized structures, except the zinc atoms coordinated by amines, other zinc atoms are all coordinated by the amide oxygen atom. Such a coordination mode was actually found for zinc trisporphyrinate as well.[29]

As shown in Figure 9A, for the free host [Zn_2-**III**], the optimized structure is in low symmetry, which leads to a conformer with a noncentrosymmetric (chiral) configuration. Such conformers exist as a pair of enantiomers, namely, the conformers A and B. For the conformer A, the two porphyrin subunits adopt an anticlockwise twist; for the conformer B, the two porphyrin subunits adopt a clockwise twist. However, the solution consists of a racemic mixture, which is optically inactive.

When the chiral guest **1R** is mixed with the host, both conformers A and B could interact with it and form the corresponding 1:1 complexes, the conformer A·**1R** and the conformer B·**1R**. Their optimized structures are shown in Figure 9B. In both cases, coordination and hydrogen-bonding interactions are maintained like those in the crystal structure. The calculations suggest that the conformer A·**1R** is more energetically favorable, which is 1.96 kJ/mol lower than the conformer B·**1R**.

DOI: 10.1021/acs.inorgchem.7b00815
Inorg. Chem. XXXX, XXX, XXX−XXX

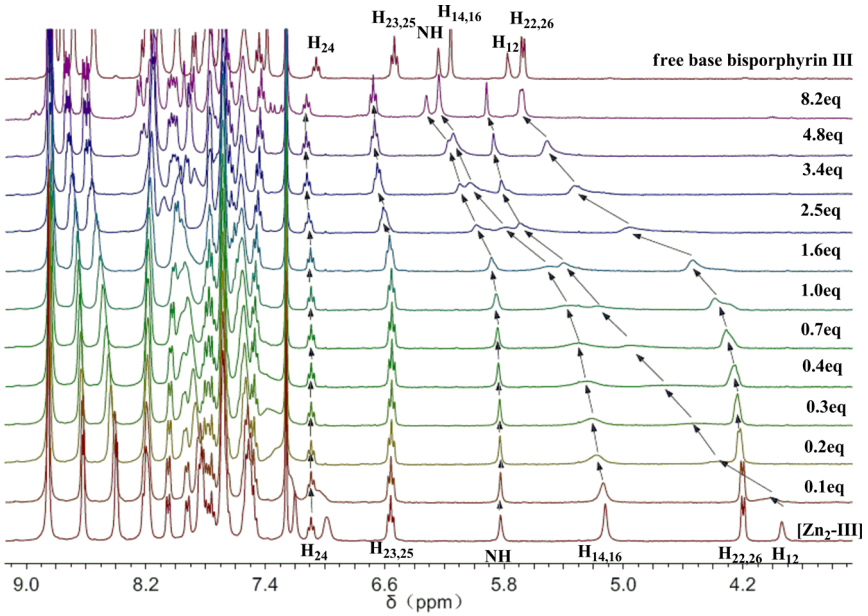

Figure 6. ^{1}H NMR spectral changes of [Zn_2-**III**] (4.4×10^{-3} M) upon the addition of **1R** in $CDCl_3$ at 298 K as the host–guest molar ratios are from 1:0 to 1:8.2.

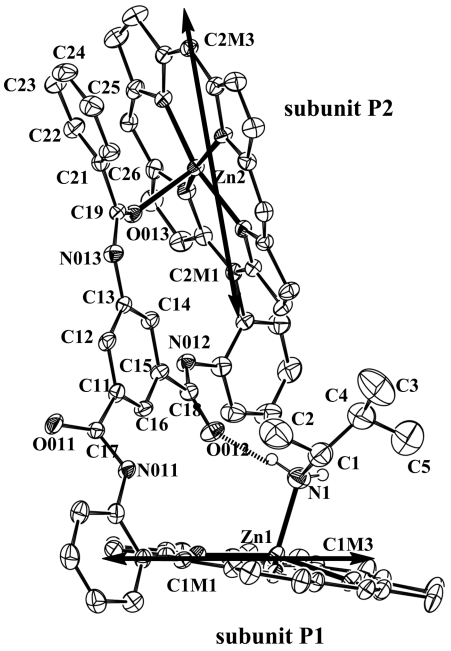

Figure 7. ORTEP view for [Zn_2-**III**]·**1R** with 50% probability thermal ellipsoids. A hydrogen bond is shown as a dashed line. The arrows show the direction of the effective transition moments along the C5···C15 axis (here labeled as C1M1···C1M3 and C2M1···C2M3). Some phenyl rings and some hydrogen atoms have been omitted for clarity.

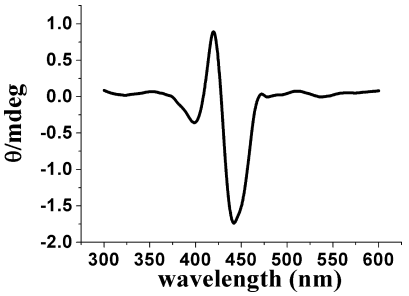

Figure 8. CD spectrum of the single crystal of [Zn_2-**III**]·**1R** in the KBr pellet.

What structural differences cause the difference in energy for these two conformers? For the chiral monoamines used in this work, the chirogenic carbon center is bonded to four different groups: NH_2, CH_3, H, and X. For the case of **1R**, X is an isopropyl group [$CH(CH_3)_2$], an alkyl substituent. Because of the coordination interaction, the position of NH_2 is fixed. Then the major differences are caused by the orientations of the other three groups. The bulkiness order is H < CH_3 < $CH(CH_3)_2$. When the guest **1R** is coordinated to zinc porphyrinate, two parts of the steric repulsions have to be considered: (1) One is between the guest and the porphyrin plane. (2) Another is between the guest and the linker. In order to minimize the steric repulsions between the guest and the porphyrin plane, in both conformers A·**1R** and B·**1R**, the least bulky group (hydrogen) is facing the porphyrin plane and the bulkiest group (isopropyl) is away from the porphyrin plane. However, as shown in Figure 9B, the orientations of the isopropyl groups in two conformers are different. In the conformer A·**1R**, it is away from the linking phenyl. However, in the conformer B·**1R**, it tilts toward the linking phenyl. The former orientation may cause less steric repulsion between the guest and the linker and lower its energy. Therefore, the conformer A·**1R** should be the major contributor to the CD spectra.

In the conformer A·**1R**, the two porphyrin subunits adopt an anticlockwise twist with a C5–C15–C5′–C15′ torsion angle of −144°. On the basis of the exciton chirality method,[28] this anticlockwise twist will lead to a negative Cotton effect. This is also consistent with our experimental results.

When the 1:1 complex further reacts with a guest, both conformers A·(**1R**)$_2$ and B·(**1R**)$_2$ of the 1:2 complexes will form. As shown in Figure 9C, in the optimized structures, the two guest molecules are not equivalent. One is similar to that in the 1:1 complex; besides the coordination interaction, it also forms a hydrogen bond with the A-type carbonyl oxygen atom. The second replaces the coordination site of the B-type

DOI: 10.1021/acs.inorgchem.7b00815
Inorg. Chem. XXXX, XXX, XXX–XXX

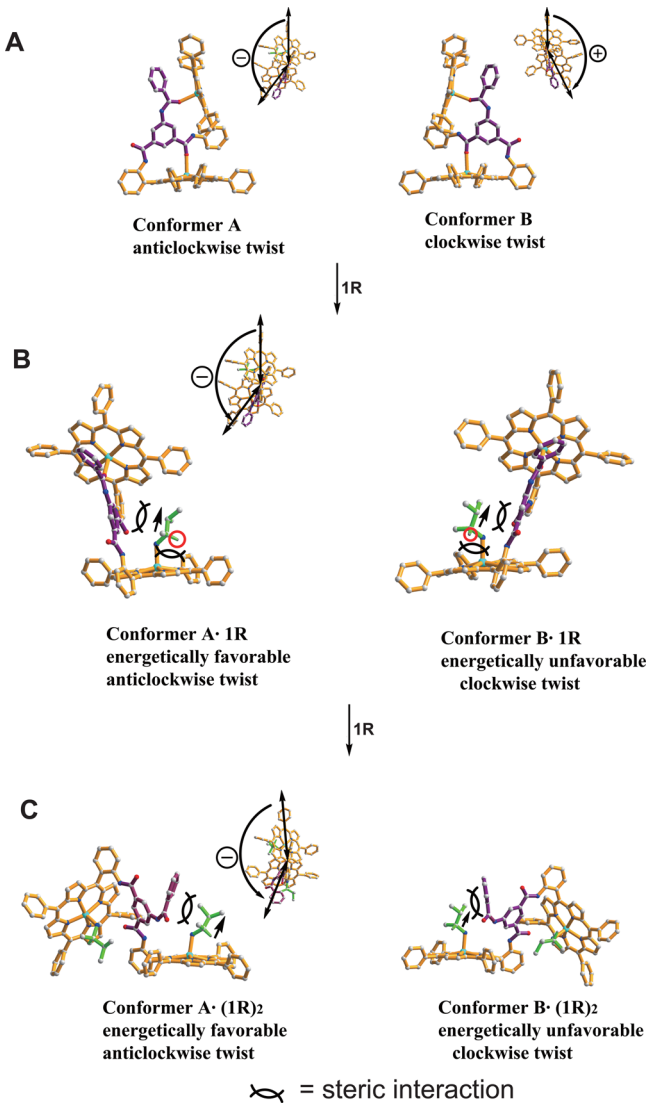

Figure 9. Chirality transfer mechanism based on DFT calculations for **1R**. Hydrogen atoms of the chiral carbon atoms are marked by red circles; arrows show the orientations of the isopropyl groups. (A) Host [Zn_2-**III**], which exists as a pair of enantiomers in solution. The conformer A forms an anticlockwise twist, and the conformer B forms a clockwise twist. (B) Optimized 1:1 host–guest complexes for [Zn_2-**III**]·**1R**. The conformer A·**1R** is more energetically favorable, which leads to the anticlockwise twist. (C) Optimized 1:2 host–guest complex for [Zn_2-**III**]·$(\mathbf{1R})_2$. The conformer A·$(\mathbf{1R})_2$ is more energetically favorable, which leads to the anticlockwise twist.

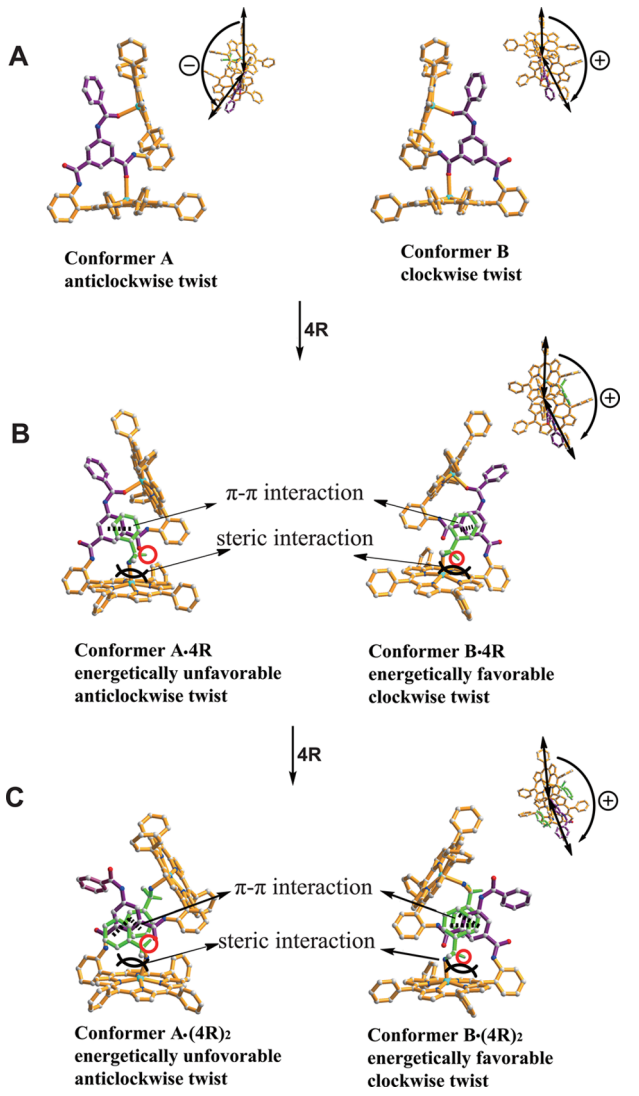

Figure 10. Chirality transfer mechanism based on DFT calculations for **4R**. Hydrogen atoms of the chiral carbon atoms are marked by red circles. (A) Host [Zn_2-**III**] existing as a pair of enantiomers, the conformers A and B. (B) Optimized 1:1 host–guest complexes for [Zn_2-**III**]·**4R**. The conformer B·**4R** is more energetically favorable, which leads to the clockwise twist. (C) Optimized 1:2 host–guest complex for [Zn_2-**III**]·$(\mathbf{4R})_2$. The conformer B·$(\mathbf{4R})_2$ is more energetically favorable, which leads to the clockwise twist.

carbonyl oxygen atom but does not form any hydrogen bond. The calculations suggest that the conformer A·$(\mathbf{1R})_2$ is more energetically favorable, which is 3.96 kJ/mol lower than the conformer B·$(\mathbf{1R})_2$. Similar to the case of their 1:1 complex, the difference could be also caused by the orientations of the isopropyl groups. Besides the different orientations of the isopropyl group of the first guest coordinated in the subunit P1, the isopropyl group of the second guest coordinated in the subunit P2 also adopts different orientations in both conformers. As shown in Figure 9C, in the conformer A·$(\mathbf{1R})_2$, the isopropyl group is away from the benzylamide substituent. However, in the conformer B·$(\mathbf{1R})_2$, it tilts toward this substituent. The former orientation may cause less steric repulsions and lower its energy. Therefore, the conformer A·$(\mathbf{1R})_2$ should be the major contributor to the CD spectra. In the conformer A·$(\mathbf{1R})_2$, the two porphyrin subunits adopt an anticlockwise twist with a C5–C15–C5′–C15′ torsion angle of −157°. On the basis of the exciton chirality method,[28] this anticlockwise twist will lead to a negative Cotton effect. This is also consistent with our experimental results.

Why are the signs of the CD signals different when the substituent is an aryl group compared to an alkyl group? In the calculations, (*R*)-1-phenylethylamine (**4R**) was used as the guest with an aryl substituent. When the chiral guest **4R** is mixed with the host, this leads to 1:1 and 1:2 complexes. For the 1:1 complexes, the optimized structures are the conformer A·**4R** and the conformer B·**4R**, as shown in Figure 10B. In both cases, hydrogen bonds are maintained. However, different from the case of **1R**, there are also $\pi-\pi$ interactions between the phenyl ring of the guest and the phenyl ring of the linker. Such types of $\pi-\pi$ interactions were also found in the reported

DOI: 10.1021/acs.inorgchem.7b00815
Inorg. Chem. XXXX, XXX, XXX–XXX

amide-linked zinc trisporphyrinate complex.[17] The calculations suggest that the conformer B·**4R** is more energetically favorable, which is 6.48 kJ/mol lower than the conformer A·**4R**.

For the chiral guest **4R**, X is a phenyl group. Because of the coordination and $\pi-\pi$ interactions, the positions of NH_2 and the phenyl group are fixed, and then the major differences between the conformer A·**4R** and the conformer B·**4R** are caused by the orientations of the methyl group and the hydrogen atom. The bulkiness order is H < CH_3. In their optimized structures, as shown in Figure 10B, the methyl group is facing the porphyrin plane in the conformer A·**4R**, while it is away from the porphyrin plane in the conformer B·**4R**. Such an orientation may cause less steric repulsion for the conformer B·**4R** and, hence, lower its energy. Therefore, the conformer B·**4R** could be the major contributor for the CD signal. In the conformer B·**4R**, the two porphyrin subunits adopt a clockwise twist with a C5−C15−C5′−C15′ torsion angle of 154°. On the basis of the exciton chirality method,[28] the above conformer will lead to a positive Cotton effect.

When both conformers of the 1:1 complex further react with a guest, both conformers A·$(\mathbf{4R})_2$ and B·$(\mathbf{4R})_2$ of the 1:2 complexes will form. As shown in Figure 10C, the two guest molecules in the optimized structures are not equivalent. One is similar to that in the 1:1 complex; besides coordination interaction, it also involves hydrogen-bonding and $\pi-\pi$ interactions. The other one only involves coordination and $\pi-\pi$ interactions but does not form any hydrogen bonds. The calculations suggest that the conformer B·$(\mathbf{4R})_2$ is more energetically favorable, which is about 0.92 kJ/mol lower than the conformer A·$(\mathbf{4R})_2$. Similar to the case of their 1:1 complex, the difference could also be caused by the orientations of the methyl group and hydrogen, as shown in Figure 10C. The methyl group is facing the porphyrin plane in the conformer A·$(\mathbf{4R})_2$, while it is away from the porphyrin plane in the conformer B·$(\mathbf{4R})_2$. Such an orientation may cause less steric repulsion for the conformer B·$(\mathbf{4R})_2$ and, hence, lower its energy. In the conformer B·$(\mathbf{4R})_2$, the two porphyrin subunits adopt an anticlockwise twist with a C5−C15−C5′−C15′ torsion angle of 168°. On the basis of the exciton chirality method,[28] this clockwise twist will lead to a positive Cotton effect. This is also consistent with our experimental results.

CONCLUSION

In conclusion, we have designed and synthesized a new *m*-phthalic diamide-linked zinc bisporphyrinate. It can function as a chirality probe for a series of chiral monoamines. For the chiral monoamines with the same handedness, the signs of their CD signals for those with an aryl group as the substituent (X) are opposite to those with an alkyl group as the substituent. NMR studies suggest that stepwise coordination leads to the 1:1 and 1:2 complexes. The crystal structure of a 1:1 host−guest complex reveals that this bisporphyrin adopts a trans configuration and the NH_2 of the amine is involved in both coordination and hydrogen-bonding interactions. DFT calculations suggest that, in the host−guest complexes, the nature of the bulkiest group X makes a difference. When X is an alkyl group, the steric repulsion causes the conformer B·**1R** to be more energetically favorable, which leads to a clockwise twist; when X is an aryl group, it can form $\pi-\pi$ interactions with the phenyl ring of the linker, which causes the conformer A·**4R** to be more energetically favorable and leads to an anticlockwise twist. Our studies suggest that, in this bisporphyrin system, the interactions between the linker and guests are crucial, and we could control chirality transfer by adjusting the linker. Further studies on the functionalization of the linker are under investigation.

ASSOCIATED CONTENT

Supporting Information

The Supporting Information is available free of charge on the ACS Publications website at DOI: 10.1021/acs.inorgchem.7b00815.

CD, UV−vis, and NMR spectra, calculation data, relative energies, and Cartesian coordinates (PDF)

Accession Codes

CCDC 1531702 contains the supplementary crystallographic data for this paper. These data can be obtained free of charge via www.ccdc.cam.ac.uk/data_request/cif, or by emailing data_request@ccdc.cam.ac.uk, or by contacting The Cambridge Crystallographic Data Centre, 12 Union Road, Cambridge CB2 1EZ, UK; fax: +44 1223 336033.

AUTHOR INFORMATION

Corresponding Authors

*E-mail: yowang@suda.edu.cn.
*E-mail: cjhu@suda.edu.cn.
*E-mail: jplang@suda.edu.cn.

ORCID

Chuanjiang Hu: 0000-0001-7126-3789
Jianping Lang: 0000-0003-2942-7385

Notes

The authors declare no competing financial interest.

ACKNOWLEDGMENTS

We thank the National Nature Science Foundation of China for financial support (Grants 21271133, 21305098, and 21531006), the Natural Science Foundation of Jiangsu Province (Grant BK2016127502), and the Local Joint Engineering Laboratory for Novel Functional Polymeric Materials and the Priority Academic Program Development of Jiangsu Higher Education Institutions. The authors are grateful for the useful comments of the Editor and reviewers.

REFERENCES

(1) Hembury, G. A.; Borovkov, V. V.; Inoue, Y. Chirality-Sensing Supramolecular Systems. *Chem. Rev.* **2008**, *108*, 1−73.
(2) Berova, N.; Pescitelli, G.; Petrovic, A. G.; Proni, G. Probing molecular chirality by CD-sensitive dimeric metalloporphyrin hosts. *Chem. Commun.* **2009**, 5958−5980.
(3) Liu, M. H.; Zhang, L.; Wang, T. Y. Supramolecular Chirality in Self-Assembled Systems. *Chem. Rev.* **2015**, *115*, 7304−7397.
(4) Borovkov, V. Supramolecular Chirality in Porphyrin Chemistry. *Symmetry* **2014**, *6*, 256−294.
(5) Rosaria, L.; D'Urso, A.; Mammana, A.; Purrello, R. Chiral memory: induction, amplification, and switching in porphyrin assemblies. *Chirality* **2008**, *20*, 411−419.
(6) Borovkov, V. V.; Hembury, G. A.; Inoue, Y. Origin, Control, and Application of Supramolecular Chirogenesis in Bisporphyrin-Based Systems. *Acc. Chem. Res.* **2004**, *37*, 449−459.
(7) Kurtan, T.; Nesnas, N.; Li, Y.-Q.; Huang, X.; Nakanishi, K.; Berova, N. Chiral Recognition by CD-Sensitive Dimeric Zinc Porphyrin Host. 1. Chiroptical Protocol for Absolute Configurational Assignments of Monoalcohols and Primary Monoamines. *J. Am. Chem. Soc.* **2001**, *123*, 5962−5973.
(8) Kurtan, T.; Nesnas, N.; Koehn, F. E.; Li, Y.-Q.; Nakanishi, K.; Berova, N. Chiral Recognition by CD-Sensitive Dimeric Zinc

DOI: 10.1021/acs.inorgchem.7b00815
Inorg. Chem. XXXX, XXX, XXX−XXX

Porphyrin Host. 2. Structural Studies of Host-Guest Complexes with Chiral Alcohol and Monoamine Conjugates. *J. Am. Chem. Soc.* **2001**, *123*, 5974−5982.
(9) Tanasova, M.; Yang, Q.; Olmsted, C. C.; Vasileiou, C.; Li, X.; Anyika, M.; Borhan, B. An Unusual Conformation of α-Haloamides Due to Cooperative Binding with Zincated Porphyrins. *Eur. J. Org. Chem.* **2009**, *2009*, 4242−4253.
(10) Borovkov, V. V.; Lintuluoto, J. M.; Fujiki, M.; Inoue, Y. Temperature Effect on Supramolecular Chirality Induction in Bis(zinc porphyrin). *J. Am. Chem. Soc.* **2000**, *122*, 4403−4407.
(11) Borovkov, V. V.; Lintuluoto, J. M.; Inoue, Y. Supramolecular Chirogenesis in Zinc Porphyrins: Mechanism, Role of Guest Structure, and Application for the Absolute Configuration Determination. *J. Am. Chem. Soc.* **2001**, *123*, 2979−2989.
(12) Anyika, M.; Gholami, H.; Ashtekar, K. D.; Acho, R.; Borhan, B. Point-to-Axial Chirality Transfer-A New Probe for "Sensing" the Absolute Configurations of Monoamines. *J. Am. Chem. Soc.* **2014**, *136*, 550−553.
(13) Jiang, J.; Feng, Z.; Liu, B.; Hu, C.; Wang, Y. Chiral recognition of amino acid esters by a novel oxalic amide-linked bisporphyrin. *Dalton Trans.* **2013**, *42*, 7651−7659.
(14) Jiang, J.; Fang, X.; Liu, B.; Hu, C. m-Phthalic Diamide-Linked Zinc Bisporphyrinate: Spontaneous Resolution of Its Crystals and Its Application in Chiral Recognition of Amino Acid Esters. *Inorg. Chem.* **2014**, *53*, 3298−3306.
(15) Liu, B.; Jiang, J.; Fang, X.; Hu, C. Absolute Configurational Assignments of Amino Acid Esters by a CD-Sensitive Malonamide-Linked Zinc Bisporphyrinate Host. *Chin. J. Chem.* **2014**, *32*, 797−802.
(16) Fang, X. S.; Han, Z.; Xu, C. L.; Li, X. H.; Wang, Y.; Hu, C. J. Discrimination between alkyl and aryl substituents of chiral monoamines by m-phthalic diamide-linked zinc bisporphyrinates. *Dalton Trans.* **2015**, *44*, 12511−12515.
(17) Han, Z.; Li, L.; Shi, B.; Fang, X. S.; Wang, Y.; Hu, C. J. Crystallographic and Spectroscopic Studies of a Host-Guest Complex Consisting of a Novel Zinc Trisporphyrinate and a Chiral Monoamine. *Inorg. Chem.* **2016**, *55*, 3730−3737.
(18) Sheldrick, G. M. Crystal structure refinement with SHELXL. *Acta Crystallogr., Sect. C: Struct. Chem.* **2015**, *71*, 3−8.
(19) Spek, A. L. *Acta Crystallogr., Sect. C: Struct. Chem.* **2015**, *71*, 9−18.
(20) Frisch, M. J.; Trucks, G. W.; Schlegel, H. B.; Scuseria, G. E.; Robb, M. A.; Cheeseman, J. R.; Scalmani, G.; Barone, V.; Mennucci, B.; Petersson, G. A.; Nakatsuji, G. H.; Caricato, M.; Li, X.; Hratchian, H. P.; Izmaylov, A. F.; Bloino, J.; Zheng, G.; Sonnenberg, J. L.; Hada, M.; Ehara, M.; Toyota, K.; Fukuda, R.; Hasegawa, J.; Ishida, M.; Nakajima, T.; Honda, Y.; Kitao, O.; Nakai, H.; Vreven, T.; Montgomery, J. A., Jr.; Peralta, J. E.; Ogliaro, F.; Bearpark, M.; Heyd, J. J.; Brothers, E.; Kudin, K. N.; Staroverov, V. N.; Kobayashi, R.; Normand, J.; Raghavachari, K.; Rendell, A.; Burant, J. C.; Iyengar, S. S.; Tomasi, J.; Cossi, M.; Rega, N.; Millam, J. M.; Klene, M.; Knox, J. E.; Cross, J. B.; Bakken, V.; Adamo, C.; Jaramillo, J.; Gomperts, R.; Stratmann, R. E.; Yazyev, O.; Austin, A. J.; Cammi, R.; Pomelli, C.; Ochterski, J. W.; Martin, R. L.; Morokuma, K.; Zakrzewski, V. G.; Voth, G. A.; Salvador, P.; Dannenberg, J. J.; Dapprich, S.; Daniels, A. D.; Farkas, Ö.; Foresman, J. B.; Ortiz, J. V.; Cioslowski, J.; Fox, D. J. *Gaussian09*, revision C.01; Gaussian, Inc.: Wallingford, CT, 2010.
(21) Borovkov, V. V.; Lintuluoto, J. M.; Sugeta, H.; Fujiki, M.; Arakawa, R.; Inoue, Y. Supramolecular Chirogenesis in Zinc Porphyrins: Equilibria, Binding Properties, and Thermodynamics. *J. Am. Chem. Soc.* **2002**, *124*, 2993−3006.
(22) Nardo, J. V.; Dawson, J. H. Magnetic circular dichroism spectroscopy as a probe of axial ligation in porphyrin complexes: zinc(II) tetraphenylporphyrin complexes with oxygen and nitrogen donor ligands. *Spectrosc.: Int. J.* **1983**, *2*, 326.
(23) Ingham, K. C. On the application of Job's method of continuous variation to the stoichiometry of protein-ligand complexes. *Anal. Biochem.* **1975**, *68*, 660−663.
(24) Gil, V. M. S.; Oliveira, N. C. On the use of the method of continuous variations. *J. Chem. Educ.* **1990**, *67*, 473−478.
(25) Ulatowski, F.; Dąbrowa, K.; Bałakier, T.; Jurczak, J. Recognizing the Limited Applicability of Job Plots in Studying Host−Guest Interactions in Supramolecular Chemistry. *J. Org. Chem.* **2016**, *81*, 1746−1756.
(26) Matile, S.; Berova, N.; Nakanishi, K.; Fleischhauer, J.; Woody, R. W. Structural Studies by Exciton Coupled Circular Dichroism over a Large Distance: Porphyrin Derivatives of Steroids, Dimeric Steroids, and Brevetoxin B. *J. Am. Chem. Soc.* **1996**, *118*, 5198−5206.
(27) Pescitelli, G.; Gabriel, S.; Wang, Y. K.; Fleischhauer, J.; Woody, R. W.; Berova, N. Theoretical analysis of the porphyrin-porphyrin exciton interaction in circular dichroism spectra of dimeric tetraarylporphyrins. *J. Am. Chem. Soc.* **2003**, *125*, 7613−7628.
(28) Berova, N.; Polavarapu, P. L.; Nakanishi, K.; Woody, R. W. *Comprehensive Chiroptical Spectroscopy*; John Wiley & Sons, Inc.: Hoboken, NJ, 2012.
(29) Li, L.; Hu, C. J.; Shi, B.; Wang, Y. Rationalization of chirality induction and inversion in a zinc trisporphyrinate by a chiral monoalcohol. *Dalton Trans.* **2016**, *45*, 8073−8080.

DOI: 10.1021/acs.inorgchem.7b00815
Inorg. Chem. XXXX, XXX, XXX−XXX